

Paper Title: The evaluation of redundancy for road traffic networks

Authors: **Rawia Ahmed EL Rashidy**, Corresponding author, Institute of Railway Research,
University of Huddersfield, Huddersfield, HD1 3DH, UK,
Email: r.elrshidy@hud.ac.uk.

Dr Susan Grant-Muller, Institute for Transport Studies, University of Leeds,
Leeds, LS2 9JT, UK, Email: s.m.grant-muller@its.leeds.ac.uk.

THE EVALUATION OF REDUNDANCY FOR ROAD TRAFFIC NETWORKS

Submitted 18 June 2014; accepted Day Month Year

Abstract. This paper presents two redundancy indices for road traffic network junctions and also an aggregated network redundancy index. The proposed redundancy indices could be implemented to identify optimal design alternatives during the planning stage of the network junctions whereas the aggregated network redundancy index could assess the best control and management policies under disruptive events. Furthermore, effective measures of network redundancy are important to policy makers in understanding the current resilience and future planning to mitigate the impacts of greenhouse gases. The proposed junction indices cover the static aspect of redundancy, i.e. alternative paths, and the dynamic feature of redundancy reflected by the availability of spare capacity under different network loading and service level.

The proposed redundancy indices are based on the entropy concept, due to its ability to measure the system configuration in addition to being able to model the inherent uncertainty in road transport network conditions. Various system parameters based on different combinations of link flow, relative link spare capacity and relative link speed were examined. However, the two redundancy indices developed from the combined relative link speed and relative link spare capacity showed strong correlation with junction delay and volume capacity ratio of a synthetic road transport network of Delft city. Furthermore, the developed redundancy indices responded well to demand variation under the same network conditions and supply variations. Another case study on Junction 3A in M42 motorway near Birmingham demonstrated that the developed redundancy index is able to reflect the impact of the Active Traffic Management scheme introduced in 2006.

Keywords: Redundancy, road traffic networks, entropy, disruptive events, active traffic management.

Introduction

The importance of redundancy has been highlighted in many disciplines. For example Downer (2009) argued that redundancy in technical systems should be understood as a ‘design paradigm’ as redundancy not only allows designers to design for high reliability, but it also permits them to quantitatively demonstrate reliability. According to Downer (2009), in engineering literature redundancy could be used as an indicator for reliability because it offers ‘a powerful and convincing rubric’ with which engineers could mathematically establish reliability levels much higher than they could derive from lab testing. Furthermore, Javanbarg and Takada (2007) highlighted the importance in assessing the redundancy of water networks from three perspectives. Firstly, it is very important to consider the redundancy in the network design stage to obtain the optimum network layout. Secondly, the insufficiency of redundancy could have a significant impact on the road transport network level of service, in addition to catastrophic consequences in the case of rapid evacuation (Immers *et al.* 2004). The third advantage according to Javanbarg and Takada (2007) is that the consideration of redundancy could help in finding the best recommended mitigation plans against different kind of disruptions.

Redundancy has a significant impact on the resilience of road transport networks as it represents the spare capacity of road transport networks under different scenarios (Lhomme *et al.* 2012). The link between redundancy and resilience concepts has been discussed in various disciplines. For example, Haimés (2009) suggested that a water distribution system could be resilient against a major storm that would shut down one of the power lines if it has redundancy in its electric power subsystem, whereas, Yazdani and Jeffrey (2012) considered redundancy along with the connectivity as the topological aspects of water network resilience. In computer science, Randles *et al.* (2011) reported that distributed redundancy improves complex system resilience and Anderson *et al.* (2011) suggested that the redundancy of road transport network is one of the resilience indicators.

The main aim of this paper is to propose a redundancy index that is able to account for the topology characteristics of road transport networks and the dynamic nature of traffic flow, while maintaining the advantages of easy implementation. The entropy concept that has been used in various disciplines to model redundancy has been employed for the first time, to develop road transport network redundancy indices. The paper initially presents a general review of the interpretation of redundancy in different disciplines. The

development of the proposed redundancy index is then described along with a discussion of the entropy concept and its use in transport applications. Two case studies are given in order to investigate the implementation of the proposed redundancy index and to test its variations under different scenarios. The methodology also explores the need to develop an aggregated redundancy index in order to evaluate the redundancy of the overall network under different conditions.

1. Survey of redundancy measures

The concept of redundancy is well established in technological fields such as engineering, computer science, and system design (Streeter, 1992). According to Streeter (1992), the redundancy characteristic of a system refers to its ability to self-organize, e.g. a process whereby internal structure and functions re-adjust along with changing circumstances. In engineering systems however, the redundancy of a system could be defined as the extent of degradation the system can suffer without losing some specified elements of its functionality (Kanno and Ben-Haim, 2011). Meanwhile, in the transport context it is defined as the availability of several paths for each set of origin destination (OD) pairs in the road transport network. Moreover, Immers *et al.* (2004) used the redundancy concept to refer to the degree of spare capacity in the network. Meanwhile, Javanbarg and Takada (2007) suggested that the redundancy of the water distribution system does not only imply the availability of several paths but also includes the excess capacity, known in the literature as the spare capacity of the network. Furthermore, (Snelder *et al.*, 2012) suggested two types of redundancy: active and passive redundancy. According to Snelder *et al.* (2012), alternative routes could be considered as ‘active redundancy’ that could be preserved under regular conditions by various measures such as road pricing or speed adjustments. For example, the M42 active traffic management (ATM) project increases the capacity and reduces the variability of journey times by allowing the use of the hard shoulder between J3a and J7 together with variable mandatory speed limits during periods of peak demand (Sultan *et al.*, 2008a). Passive redundancy could be used to represent back-up options that are only used in case of disruptions. As a specific example, the use of fast train services, ferries, coaches to travel across Europe as a result of airline disruptions during the 2010 Eyjafjallajökull Volcano (eTN, 2010). Furthermore, Immers *et al.* (2004) explained that redundancy could be a multi-level concept as follows:

- Strategic level: coordination between activity patterns such as avoiding major road works during peak period or organized events.
- Tactical level: coordination amongst multimodal transport services and networks, similar to passive redundancy explained above. This is also known as ‘dis-

tributed redundancy’ where different systems could deliver the same outcomes (Randles *et al.*, 2011).

- Operational level: to manage the supply-demand relationships in the road transport network by applying different intelligent transport systems (ITS). For example using variable message signs to advise travellers on alternative routes in the case of link closure due to an accident.

Despite the importance of redundancy at both strategic and tactical levels, the current research focuses on proposing an indicator to quantify the operational redundancy of the road transport network (i.e. active redundancy) that could feed into both levels. It has been noted that there is a lack of research into the redundancy concept in the case of road transport networks compared with other networks, such as water distribution networks and power networks. For example there are several indices (Yazdani, Jeffrey 2012; Javanbarg and Takada, 2007; Awumah *et al.* 1991; Hoshiya *et al.* 2004) that have been developed to investigate the redundancy in the water distribution network using the entropy concept.

In the road transport network, the redundancy concept could be evaluated by considering the static conditions of the network such as road density. Jenelius (2009) pointed out that a higher road density to some extent guarantees a higher availability of alternative paths. However road density only reflects the impact of the supply side without considering the effect of changes in demand and traffic conditions. Furthermore, road density only considers the fully-operational link status e.g. by adding the link length to the whole network length or subtracting link length when the link is fully closed. Hyder (2010) estimated the redundancy value of a link as the total number of motorways, A roads, and B roads¹ within a 10 kilometre radius of the link. However, both approaches (i.e. Hyder, 2010; Jenelius, 2009) introduced static, purely topological indicators. They do not indicate the impact of different traffic conditions (e.g. the road density, or the number of adjacent routes despite the traffic flow conditions of the alternatives) in estimating the redundancy of the link.

Graph theory has also been used to quantify the redundancy of networks by using a number of indices, such as a clustering coefficient and the number of independent routes (Boccaletti *et al.*, 2006). The clustering coefficient, also known as transitivity, is a measure of redundancy as it represents the overall probability for the network to have interconnected adjacent nodes (Rodrigue *et al.*, 2009), which could be measured by different indicators (Boccaletti *et al.*, 2006). The clustering coefficient is a significant characteristic of road transport network redundancy, however, it only considers the directly neighbouring nodes or links and neglects possible capacity limitations which may restrict redundancy (Erath *et al.*, 2009). Similarly, the number of independent routes is not an ideal measure of network redundancy as it is purely a topological measure and is based

¹ A roads – “major roads intended to provide large-scale transport links within or between areas; B roads – roads intended to connect different areas, and to feed traffic between A roads and smaller roads on the network” (DfT 2011).

on an arbitrary threshold (Corson, 2010).

Jenelius (2010) introduced a “redundancy importance” concept as a new way to study the role of the link in network redundancy. The author quantified the importance of redundancy in two ways. Firstly, the importance of flow based redundancy was calculated as the weighted sum of the difference in flow arising from the closure of all links in the network. Secondly, an impact based redundancy importance measure was computed as the weighted sum of the difference in the impact measure arising from the closure of all links in the network.

The above discussion highlights the lack of redundancy research in the transport context compared with the case for water distribution networks and power grids. Furthermore, the redundancy index developed should be able to account for the topological characteristics of road transport networks as well as the dynamic nature of traffic flow.

2. A redundancy model

Based on the previous discussion, the quantification of redundancy requires both traffic flow variations and network topology to be taken into account. In this research, the level of redundancy has been investigated at the ‘node to node’ level rather than at ‘zone to zone’. By doing so, it is possible to identify critical nodes within the network that have low redundancy indices and their impact on the overall network redundancy. The proposed model of redundancy can, then, assist policy makers to evaluate the effectiveness of particular policies or to assess the impact of the implementation of new technologies, for example the Active Traffic Management scheme introduced at Junction 3A in M42 motorway (See the second case study below).

There are many uncertainties associated with road transport networks under different operational conditions. These include the uncertainties related to the supply side (such as link flow under different operational conditions) in addition to uncertain demand. To deal with these uncertainties, the concept of information entropy is adopted as one way of measuring uncertainty in the road transport network. In the following section a brief introduction to the entropy concept is given, followed by an outline of its use in modelling systems.

2.1 The entropy concept

The concept of entropy was initially proposed by Shannon (1948) to investigate the performance of communication channels and measure the uncertainties. The generic form of the entropy is as follows;

$$H(x) = \sum_{i=1}^n p_i \ln(1/p_i) \quad (1)$$

where: $H(x)$ is an entropic measure of a system x , n is the total number of the system elements under consideration and p_i represents a system parameter that could be used to identify a certain characteristic of element i . According to Swanson *et al.* (1997), the entropy measure suggested by Shannon (1984) is a good measure to quantify the existing number of degrees of freedom of a system. In general, the relative link flow is used as a system parameter (Javanbarg and Takada 2007). For example, if a node (J)

has a number of adjacent links (l), then p_i could be the relative flow of link (i), e.g. flow f_i of link i divided by the total flow of node J , i.e. $p_i = f_i / \sum_{k=1}^l f_k$.

According to Wilson (1970) there are two main streams in the use of the entropy concept; namely a measure of some property of a system and a model building tool to maximise the available information. For example, the entropy concept is used widely in water distribution networks (Hoshiya *et al.*, 2002), power grids (Koc *et al.*, 2013) and computer networks (Randles *et al.*, 2011). In transport literature, the entropy concept is widely accepted as a subjective measure to develop a trip distribution model using entropy-maximising methods (Wilson 1970). For example, Sun *et al.* (2011) proposed an entropy-based optimization approach to estimate the demand for transfers between the transport modes available in an intermodal transport terminal. Miao *et al.* (2011) developed an assessment model of capacity reliability for road network from the perspective of route entropy. Allesina *et al.* (2010) introduced a new quantitative measurement of complexity for a supply network using eight indices based on the entropy concept.

2.2 Junction redundancy index

Equation (1) above is used here to develop a proposed redundancy index for nodes in the road transport network. Two redundancy indices are developed for each node; an outflow redundancy index ($RI1_{out}$) and an inflow redundancy index ($RI1_{in}$). $RI1_{out}$ is estimated based on the outbound links whereas $RI1_{in}$ is calculated based on the inbound links of a node, as given in Eqs. (2) and (3) respectively, below.

$$RI1_{out}(o) = \left(\sum_{b=1}^k \frac{f_{bm}^i}{\sum_{z=1}^k f_{zm}^i} \ln \frac{\sum_{z=1}^k f_{zm}^i}{f_{bm}^i} \right) / \ln(k) \quad (2)$$

$$RI1_{in}(o) = \left(\sum_{a=1}^n \frac{f_{am}^i}{\sum_{z=1}^n f_{zm}^i} \ln \frac{\sum_{z=1}^n f_{zm}^i}{f_{am}^i} \right) / \ln(n) \quad (3)$$

where: f_{bm}^i is the outbound flow of link b during time interval i using a travel mode m , k is the total number of outbound links attached to node o , f_{am}^i is the inbound flow of link a during time interval i using a travel mode m and n is the total number of inbound links attached to node o (see Figure 1). The travel mode m indicates different highway or public transport networks; however, in this research, the focus is on the highway network. The redundancy indices in Eqs. (2) and (3) are normalized by $\ln(k)$ or $\ln(n)$ respectively, so as to have a range between 0 and 1 (Nagata and Yamamoto, 2004; Corson, 2010), provided that each link considered should have a traffic flow greater than 0 ($f_{bm}^i > 0$ and $f_{am}^i > 0$), i.e. links with zero traffic flow are not considered. The value of $RI1_{in}(o)$ or $RI1_{out}(o)$ is equal to 0 when either all traffic flow from or to node (o) is assigned to one link, whilst the maximum value of node redundancy indicator is 1, when the traffic flow is equally distributed over the attached links, as proved below.

Assuming a node o has k links where the inbound traffic flow of link i is f_i and the total inbound flow at the node is F , the inflow redundancy indicator $RI1_{in}(o)$ using Eq. (3) is:

$$RI1_{in}(o) = \left(\frac{f_1}{F} \ln \left(\frac{F}{f_1} \right) + \frac{f_2}{F} \ln \left(\frac{F}{f_2} \right) + \dots + \frac{f_n}{F} \ln \left(\frac{F}{f_n} \right) \right) / \ln(n)$$

As $0 < f_i/F \leq 1$, therefore $RI1_{in}(o) \geq 0$. When $\frac{f_i}{F} = 1$, other links are not assigned any traffic flow and $RI1_{in}(o) = 0$. Meanwhile, the maximum value of entropy is achieved when the flow over the attached links is equally distributed. In such a case, the inbound traffic flow of each link is:

$$f_1 = f_2 = \dots = f_n = \frac{F}{n}$$

Substituting the inbound traffic flow of each link in the above formula produces the inflow redundancy indicator $RI1_{in}$ as follows:

$$RI1_{in}(o) = \left(\frac{1}{n} \ln(n) + \frac{1}{n} \ln(n) + \dots + \frac{1}{n} \ln(n) \right) / \ln(n)$$

$$RI1_{in}(o) = n \left(\frac{1}{n} \ln(n) \right) / \ln(n)$$

$$RI1_{in}(o) = 1$$

The redundancy index $RI1(o)$ of a node (o) is eventually controlled by either $RI1_{in}(o)$ or $RI1_{out}(o)$. To identify the more influential redundancy index i.e. $RI1_{in}(o)$ or $RI1_{out}(o)$, the junction delay and junction volume capacity ratio are calculated for each direction (i.e. inbound and outbound) and correlated against the respective values of $RI1_{in}(o)$ or $RI1_{out}(o)$. The index most strongly correlated with these two junction levels of service identifies the junction redundancy level, as presented in section 4.1.1 below. The junction delay, $JD_{in}^i(o)$, for inbound links is calculated by the following equation:

$$JD_{in}^i(o) = \sum_{a=1}^n (t_{am}^i - T_{am}^i) f_{am}^i / \sum_{z=1}^k f_{zm}^i \quad (4)$$

where: t_{am}^i is the actual travel time for inbound link a during time interval i using travel mode m . k is the total number of inbound links and T_{am}^i is the free flow travel time of inbound link a during time interval i using travel mode m . The junction volume capacity ratio, $JVCR_{in}^i(o)$, is calculated as:

$$JVCR_{in}^i(o) = \frac{\sum_{a=1}^n f_{am}^i}{\sum_{a=1}^n C_{am}} \quad (5)$$

where: C_{am} is the design capacity of link a with mode m . Similarly, the two equations, (4) and (5) can also be adjusted to obtain junction delay and the volume capacity ratio for the outbound links.

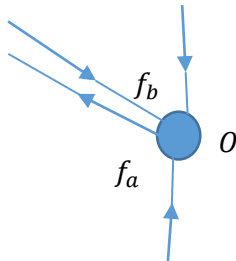


Figure 1 Example illustrating the outbound and inbound flows of node o .

2.3 Analysis and limitations of the proposed redundancy index

In this section, simple numerical examples are presented to examine the validity of the proposed $RI1_{in}$ and $RI1_{out}$ in reflecting the topological properties of the node (e.g. number of attached links) in addition to traffic flow variation. Figure 2(a) shows node J with five links (2 inbound and 3 outbound links) whilst the traffic flow for each link is also shown in Figure 2. Eqs. (2) and (3) have been used to calculate $RI1_{out}(J)$ and $RI1_{in}(J)$ as 0.96 and 0.89 respectively, reflecting the impact of the increase in the number of outbound links. However, if the number of outbound and inbound links is the same but the flow distributions are different, e.g. node (O) in Figure 2(b), $RI1_{in}(O)$ increases to 0.94 due to the change in load distribution (i.e. change from 900/400 to 830/470), whereas $RI1_{out}(O)$ significantly decreases to 0.78 due to the reduction of outbound links. This illustrates how the entropy concept reflects load distribution on the redundancy level. In general, the distribution of load between the adjacent links has a significant impact on the entropy value. A higher value of $H(x)$ presented in Eq. (1) could be obtained for the same total flow by the uniform distribution of the flow over the incident links, as concluded by Shannon (1948). For example, if the outbound flows of node Z shown in Figure 2(c) are equally distributed over the two outbound links, $RI1_{out}$ will be 1, higher than a value for $RI1_{in}$ of 0.90 in the case of a 580/270 flow distribution. Doubling the flow on each link (with the same flow distribution between links) gives the same redundancy index. For example $RI1_{in}$ for node Q (see Figure 2(d)) has the same value of 0.90 when the link flow increases to 1160 and 540 from 580 and 270, as that shown for node Z in Figure 2(c).

This shortcoming of $RI1_{out}$ and $RI1_{in}$ (defined by Eqs. (2) and (3)) highlights the need to introduce traffic flow variation compared with the link capacity in the definition of the redundancy index. In this respect the redundancy index will then incorporate the link spare capacity in line with Immers *et al.* (2004). The next section introduces alternative redundancy indices to include the impact of link traffic conditions in the calculation of the redundancy of attached nodes.

2.4 Impact of link spare capacity and travel speed on junction redundancy

To reflect the impact of increases/decreases in flow on node redundancy, the relative link spare capacity, ρ_{am}^i is introduced. For an inbound link a , ρ_{am}^i is represented by the percentage of the link spare capacity with respect to the node total spare capacity, as given by Eq. (6).

$$\rho_{am}^i = \frac{C_{am} - f_{am}^i}{\sum_{a=1}^n C_{am} - f_{am}^i} \times 100 \quad (6)$$

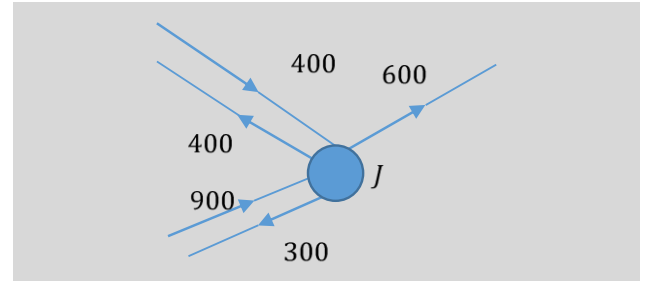
In addition to the impact of link spare capacity, link average travel speed should also be integrated to reflect the impact of the level of service on the redundancy index. As each link has its own free flow speed, the influence of link flow speed on junction redundancy is incorporated here using the relative link speed, RLS and calculated by the following equation:

$$RLS(a) = \frac{v_{am}}{V_{am}} \quad (7)$$

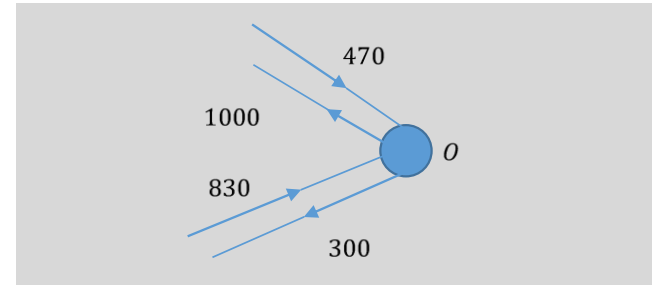
where: v_{am} is the average travel speed of link a and V_{am} is the free flow travel speed of link a .

The redundancy indices proposed here are based on different logical combinations of relative link spare capacity, ρ_{am}^i and relative link speed (RLS). The main aim is to identify the best system parameters that can be used to develop a junction redundancy index, reflecting the junction topology and traffic flow conditions. Five additional redundancy indices are therefore introduced as given in Table 1. In $RI2_{in}$ and $RI6_{in}$ the relative link spare capacity ρ_{am}^i is used as the system parameter. However, in $RI6_{in}$, the calculated entropy for each link is weighted by the relative link speed, RLS_a , to account for the dynamic flow variation. In contrast the effect of the relative link speed, RLS_a , is included in the system parameter of $RI3_{in}$. The system parameter p_i used in $RI3_{in}$ is therefore given by the multiplication of the relative link speed RLS_a by the relative link spare capacity, ρ_{am}^i . The system parameter used in $RI5_{in}$ is the relative link speed RLS_a multiplied by the relative link capacity with respect to the total junction capacity $C_{am} / \sum_{a=1}^n C_{am}$. In the final redundancy index considered, $RI4_{in}$, the relative link spare capacity ($C_{am} - f_{am}^i$) to link capacity C_{am} has been employed as the system parameter. However the calculated entropy for each link has been weighted by the relative link speed RLS_a in a similar way to $RI6_{in}$.

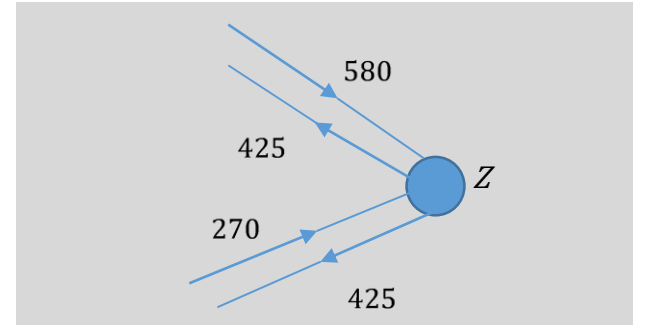
Tables 2 and 3 show the flow of links and the values of $RI1_{in}$, $RI1_{out}$, $RI2_{in}$ and $RI2_{out}$ for the four nodes presented in Figure 2 and two different road capacities of 1200 and 2200 vehicles per hour (veh/hr), respectively. Other redundancy indices are not presented in Tables 2 and 3 as their calculation requires the relative link speed value RLS . The values of each link capacity, C_{am} , could vary based on the road type and speed limit. For example, C_{am} could be equal to 1200, 1500, or 1800 veh/hr in case of urban links whereas 2200 or 2400 veh/hr is more appropriate for a motorway link type. In this numerical example, C_{am} is taken equal to 1200 (Table 2) and 2200 (Table 3) veh/hr to investigate the impact of link capacity on the redundancy indices. Taking the impact of spare capacity into account leads to a decrease in the redundancy index when the flow increases; however, its importance is highlighted when the flow doubles but has the same distribution (see Table 2).



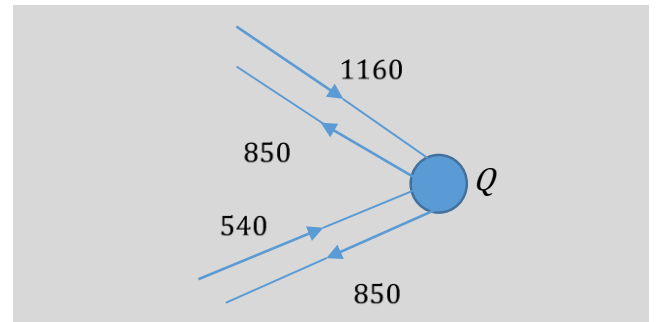
(a) Node J



(b) Node O



(c) Node Z



(d) Node Q

Figure 2 Examples illustrating different traffic flow (veh/hr) and topology properties on redundancy index.

For example in Table 2, nodes Z and Q have the same number of links but double the flow, consequently $RI2_{in}$ (Q) is decreased compared with $RI2_{in}$ (Z), whereas $RI1_{in}$ (Q) is equal to $RI1_{in}$ (Z). Furthermore, the outbound flow for both nodes, Z and Q are equally distributed over the two outbound links, leading to the same $RI1_{out}$ and $RI2_{out}$ for

the two nodes Z and Q . This reflects the ability of $RI2_{in}$ to consider the impact of flow increases, other than in the case of equally distributed flow. To investigate the impact of flow distribution on node redundancy, node (O) has an inbound flow distribution different to that of the outbound flow. This leads to different inbound and outbound redundancy indices. It has been found that the increase in a link flow compared with the other adjacent links leads to a decrease in the redundancy indices even though the total flow remains the same. To investigate the impact of the number of links adjacent to the node, node (J) has been introduced with 2 inbound links, meanwhile the number of outbound links are 3. Consequently both indices, $RI1_{out}$ and $RI2_{out}$ are higher than the inbound redundancy indices $RI1_{in}$ and $RI2_{in}$, respectively, reflecting the ability of both indices to represent the topological aspects of nodes.

Comparing Tables 2 and 3, the increase in link capacity (from 1200 to 2200 veh/hr) leads to an increase in $RI2_{in}$ and $RI2_{out}$ of different percentages, whereas $RI1_{in}$ and $RI1_{out}$ are the same for each node. For example, $RI2_{in}$ and $RI2_{out}$ of nodes (J), (O), (Z) and (Q) increase due to capacity increases and as other properties such as flow distribution and total flow remain the same.

The suitability of the redundancy indices presented in Table 1 is further applied on two case studies, namely a synthetic road transport network of Delft city and Junction 3A of the M42 motorway near Birmingham, as explained in Section 4 of the paper.

3. Network redundancy index

Despite the importance of the node redundancy based index in identifying nodes with low redundancy, there is still a need, however, for an aggregated redundancy index in order to evaluate the redundancy of the whole network under different conditions. A network redundancy indicator could be used to assess the effectiveness of different policies or technologies on the improvement of overall network redundancy. Furthermore, an evaluation of the network redundancy using a single index can help in comparing network redundancy level under different conditions, as explained in case study 1 below.

The redundancy indices, $RI_{in}(o)$ and $RI_{out}(o)$, for all the nodes in the road transport network are calculated first. A network redundancy index (NRI_{in}) is developed by summing a weighted RI_{in} for all the nodes in the network as given in Eqs. (8) and (9) below. The weight considered in the equations below is the node flow with respect to the total network flow.

$$NRI_{in} = \sum_{o=1}^N \frac{f_{om}^i}{\sum_{o=1}^N f_{om}^i} RI_{in}(o) \quad (8)$$

$$NRI_{out} = \sum_{o=1}^N \frac{f_{om}^i}{\sum_{o=1}^N f_{om}^i} RI_{out}(o) \quad (9)$$

where: f_{om}^i is the total flow of node o during the time interval i using a travel mode m and N is the total number of nodes in the road transport network.

Table 1 System parameters used in the six redundancy indices considered.

| | System parameter | Redundancy index formulation | System parameter explanation |
|------------|--|--|--|
| $RI1_{in}$ | $p_i = \frac{f_{am}^i}{\sum_{z=1}^n f_{zm}^i}$ | $RI1_{in}(o) = (\sum_{a=1}^n \frac{f_{am}^i}{\sum_{z=1}^n f_{zm}^i} \ln \frac{\sum_{z=1}^n f_{zm}^i}{f_{am}^i}) / \ln(n)$ | Link flow f_{am}^i with respect to the total junction flow $\sum_{z=1}^n f_{zm}^i$ |
| $RI2_{in}$ | $p_i = \rho_{am}^i$ | $RI2_{in}(o) = (\sum_{a=1}^n \rho_{am}^i \ln(1/\rho_{am}^i)) / \ln(n)$ | Relative link spare capacity ρ_{am}^i |
| $RI3_{in}$ | $p_i = RLS_a \rho_{am}^i$ | $RI3_{in}(o) = (\sum_{a=1}^n (RLS_a \rho_{am}^i) \ln(1/(RLS_a \rho_{am}^i))) / \ln(n)$ | Relative link speed RLS_a multiplied by relative link spare capacity ρ_{am}^i |
| $RI4_{in}$ | $p_i = \frac{C_{am} - f_{am}^i}{C_{am}}$ | $RI4_{in}(o) = (\sum_{a=1}^n RLS_a (\frac{C_{am} - f_{am}^i}{C_{am}}) \ln(\frac{C_{am}}{C_{am} - f_{am}^i})) / \ln(n)$ | Relative spare capacity $(C_{am} - f_{am}^i)$ to link capacity C_{am} . However, the calculated entropy for each link is weighted by the relative link speed RLS_a |
| $RI5_{in}$ | $p_i = RLS_a \frac{C_{am}}{\sum_{a=1}^n C_{am}}$ | $RI5_{in}(o) = (\sum_{a=1}^n (RLS_a \frac{C_{am}}{\sum_{a=1}^n C_{am}}) \ln(\frac{\sum_{a=1}^n C_{am}}{RLS_a C_{am}})) / \ln(n)$ | Relative link speed RLS_a multiplied by relative link capacity with respect to the total junction capacity $\frac{C_{am}}{\sum_{a=1}^n C_{am}}$ |
| $RI6_{in}$ | $p_i = \rho_{am}^i$ | $RI6_{in}(o) = (\sum_{a=1}^n RLS_a (\rho_{am}^i) \ln(1/\rho_{am}^i)) / \ln(n)$ | Relative link spare capacity ρ_{am}^i . However, the calculated entropy for each link is weighted by the relative link speed RLS_a |

Table 2 Redundancy indices for nodes shown in Figure 2 using $c_{am}=1200$ veh/hr.

| Node | Inbound links Flow | $RI1_{in}$ | $RI2_{in}$ | Outbound links flow | $RI1_{out}$ | $RI2_{out}$ |
|------|--------------------|------------|------------|---------------------|-------------|-------------|
| J | 900/400 | 0.89 | 0.85 | 600/400/300 | 0.96 | 0.99 |
| O | 830/470 | 0.94 | 0.92 | 1000/300 | 0.78 | 0.68 |
| Z | 580/270 | 0.90 | 0.97 | 425/425 | 1.00 | 1.00 |
| Q | 1160/540 | 0.90 | 0.32 | 850/850 | 1.00 | 1.00 |

Table 3 Redundancy indices for nodes shown in Figure 2 using $c_{am}=2200$ veh/hr.

| using Node | Inbound links flow | $RI1_{in}$ | $RI2_{in}$ | Outbound links flow | $RI1_{out}$ | $RI2_{out}$ |
|------------|--------------------|------------|------------|---------------------|-------------|-------------|
| J | 900/400 | 0.89 | 0.98 | 600/400/300 | 0.96 | 1.00 |
| O | 830/470 | 0.94 | 0.99 | 1000/300 | 0.78 | 0.96 |
| Z | 580/270 | 0.90 | 0.99 | 425/425 | 1.00 | 1.00 |
| Q | 1160/540 | 0.90 | 0.96 | 850/850 | 1.00 | 1.00 |

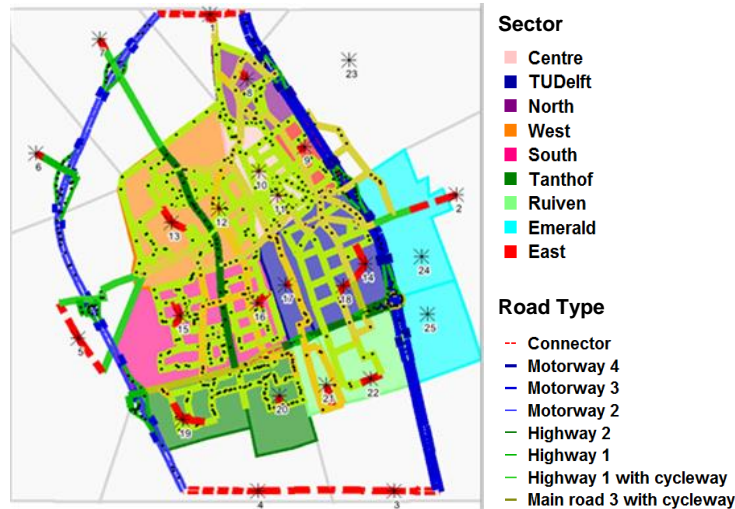


Figure 3 The synthetic road transport network of Delft city.

4. Application case studies

4.1 Case study 1: Delft road transport network

A synthetic road transport network of Delft city is used to illustrate the redundancy of road network under different scenarios using the proposed methodology. The Delft road transport network consists of 25 zones, two of which are under development (24 & 25) and 1142 links. 483 links are bi-directional and 176 are one-way including connectors and different road types as depicted in Figure 3. The Delft road transport network demonstrates a realistic network size, in addition to the availability of socioeconomic data of Delft in OmniTrans software (Version number 6.024). A full description of the Delft city road transport network is given in El Rashidy and Grant-Muller (2014), which was concerned with measuring the vulnerability of the network.

4.1.1 Redundancy indices of various nodes in Delft road network

In the case study undertaken here the OmniTrans modelling software (Version number 6.024) has been employed to obtain the spatial distribution of the traffic volume using the user equilibrium assignment (UE). UE is based on Wardrop's first principle whereby no individual trip maker can reduce his/her path cost by switching routes. This principle is also known as the user optimum (Wardrop 1952). The mathematical formulation of UE is explained in detail in (Ortúzar, Willumsen 2011). Junction modelling available in OmniTrans software is also integrated with UE model to enhance the network simulation.

The output from OmniTrans (version number 6.024) includes traffic flow in various links connected to each network node. A computer programme has been developed using MATLAB (R2011a) to calculate RI_{out} and RI_{in} for each node using the different equations presented in Table 1.

The proposed indices are calculated under the same network and traffic conditions to test the ability of the index to reflect the redundancy concept. The aim of using different performance parameters is to find out the most suitable one to develop the redundancy index. Each proposed index is calculated for each junction using Matlab code and compared with the junction delay in adjacent links. For example, the inbound redundancy index of a junction is compared with the junction delay for inbound links, whereas the outbound redundancy index of this node is compared with the junction delay of outbound links. Furthermore, in the case of a strong correlation between a redundancy index and junction delay or volume capacity ratio, each redundancy index is classified according to the junction type and investigated further. The following analysis focuses on RI_{in} only, given that there was no correlation between any RI_{out} and either the junction delay or volume capacity ratio.

Table 4 lists the correlation coefficient, r , between the proposed redundancy indices and either the junction delay or volume capacity ratio. r is a statistical measure of the degree to which two variables are linearly related. Table 4

indicates a strong correlation between the redundancy indices (RI_{2in}), (RI_{3in}) and (RI_{6in}) and both the junction delay and volume capacity ratio. In contrast, RI_{1in} and RI_{5in} exhibit a very low correlation with both the junction delay and volume capacity ratio. Furthermore, RI_{4in} is strongly positively correlated with the junction volume capacity ratio ($r=0.95$), indicating the unsuitability of RI_{4in} to model junction redundancy, as redundancy should be inversely proportional to the junction volume capacity. RI_{6in} , RI_{3in} , and RI_{2in} exhibit moderate correlation with the junction volume capacity ratio (-0.76, -0.71 and -0.69, respectively). The above analysis led to the exclusion of RI_{1in} , RI_{4in} and RI_{5in} as redundancy indices from any further analysis.

Table 5 gives a summary of r values of the remaining three redundancy indices for different junction types. In general it suggests that RI_{3in} and RI_{6in} are the most suitable redundancy indices as they can reflect junction delay and volume capacity ratio for different junction types, as indicated by the high value of r . Furthermore, the analysis of RI_{2in} based on junction type shows that there is variation from one junction type to another. For example, the highest r , 0.87, between RI_{2in} and total junction delay is for an equal priority junction type and roundabout junction type (see Table 5). The lowest value of r (=0.49) between RI_{2in} and total junction delay is for a give-way junction type, as depicted in Table 5. Similarly, the correlation between RI_{2in} and junction volume capacity ratio varies according to the junction type.

r for RI_{3in} with junction delay for all junction types is higher than those for RI_{2in} , except for the roundabout junction type (which decreases by 2.4%). The highest increase occurs for the give-way junction type, where r increases by 67% (see Table 5). Regarding the correlation between RI_{3in} and junction volume capacity ratio, two junction types (i.e. equal priority and give-way junction types), show some improvement over RI_{2in} (see Table 5). For the other two types (i.e. signalized junction and roundabout), the r value between RI_{3in} and the junction volume capacity ratio has declined compared to that between RI_{2in} and junction volume capacity ratio. Table 5 also confirms the high correlation of RI_{6in} with junction delay and junction volume capacity ratio for different junction types. Overall, Table 5 indicates that the suitability of each redundancy index relies on the junction type. However, RI_{2in} has generally a lower correlation with junction delay and the junction volume capacity ratio for different junction types than either RI_{3in} or RI_{6in} . As a result, RI_{3in} and RI_{6in} are examined further below.

In the following, both RI_{3in} and RI_{6in} are calculated for a small number of junctions from the synthetic Delft road network to show their validity. RI_{3in} and RI_{6in} have been selected as they exhibited a reasonably consistent performance for various junction types. Table 6 shows four selected junctions from the synthetic Delft road network with the flow, average speed, free flow speed and capacity of their inbound links along with the calculated values of RI_{3in} and RI_{6in} . The calculated values of both redundancy indices show the impact of spare capacity and speed variations. For example, node 5001 is connected with two inbound links with a very low traffic flow compared with

their link capacity (i.e. junction volume capacity ratio = 0.07) and average speed equal to free flow speed (junction delay = 0) exhibits a maximum value of $RI3_{in}$ (=1) and $RI6_{in}$ (=1). Node 6856 has 3 inbound links with a slightly high traffic flow compared with link capacity (=0.64) in one link, causing a reduction in its average speed (junction delay = 23.53 Veh/min and volume capacity ratio = 0.26), and therefore, $RI3_{in} = 0.91$ and $RI6_{in} = 0.88$. Furthermore, node 6983 connected with inbound links has a higher junction delay time and volume capacity ratio than node 6856, consequently, its $RI3_{in}$ and $RI6_{in}$ are lower than node 6858 redundancy indices as presented in Table 6. Furthermore, to compare the effect of the variation in junction delay and the volume capacity ratio on the redundancy indices, node 7094 was chosen as it has a higher junction delay and lower volume capacity ratio than node 6983. The calculated values of $RI3_{in}$ and $RI6_{in}$ for junction 7094 are 0.81 and 0.79 respectively. These are higher than the calculated redundancy indices for junction 6983, indicating that both indices experienced more sensitivity to the increase in junction volume capacity ratio than the increase in junction delay.

Table 4 Correlation Coefficient r of various redundancy indices with junction delay (JD) and volume capacity ratio (v/c).

| Redundancy index | JD | v/c |
|------------------|-------|-------|
| $RI1_{in}$ | 0.00 | 0.42 |
| $RI2_{in}$ | -0.71 | -0.69 |
| $RI3_{in}$ | -0.77 | -0.71 |
| $RI4_{in}$ | 0.35 | 0.95 |
| $RI5_{in}$ | -0.25 | -0.40 |
| $RI6_{in}$ | -0.77 | -0.76 |

Note: +ive and -ive correlation coefficients indicate that, as JD or v/c increases, RI increases and decreases, respectively.

4.1.2 Impact of demand variations on redundancy indices of Delft road network

The impact of variations in demand on $RI3_{in}$ and $RI6_{in}$ in addition to the network redundancy index (NRI) for the Delft road transport network was investigated using different departure rates during the morning peak. $RI3_{in}$ and $RI6_{in}$ were calculated from the equations presented in Table 1, whereas Eq. (8) is implemented to calculate the network redundancy indices $NRI3_{in}$ and $NRI6_{in}$.

Figure 4 shows the variations of $NRI3_{in}$ and $NRI6_{in}$ under uniformly distributed departure rates, whilst Figure 5 plots the variations of $NRI3_{in}$ and $NRI6_{in}$ under different departure rates. Figure 4 shows that as the load rate stays constant, $NRI3_{in}$ and $NRI6_{in}$ are also constant; however, $NRI3_{in}$ is larger than $NRI6_{in}$. Otherwise the redundancy level measured by $NRI3_{in}$ and $NRI6_{in}$ follows an opposite trend to the departure rate as depicted in Figure 5, i.e. decreases with the departure rate increase. Similarly, both network indices, $NRI3_{in}$ and $NRI6_{in}$ follow an opposite trend to the total delay (Vehicle hour) as shown in Figure 6. This leads to the conclusion that the proposed network

indices $NRI3_{in}$ and $NRI6_{in}$ are able to reflect the impact of demand variation under the same network condition.

4.1.3 Impact of supply variations on redundancy indices of Delft road network

In this analysis the ability of $NRI3_{in}$ and $NRI6_{in}$ to capture the impact of reductions in network capacity under the same variations of demand is examined. Overall network capacity could be reduced in real life conditions due to the effect of network wide events such as heavy rain or snowfall. This group of scenarios was undertaken using a reduced capacity of 2, 4 and 10% in order to model the impact of a weather related event. Figure 7 shows the variations in the network redundancy index, $NRI3$, for the variations in supply (as stated above) and the same variation in departure rate shown in Figure 5. $NRI3$ shows variations during the modelling period (7:00-9:00) in the case of reduced capacity compared with full network capacity as depicted in Figure 7. In general, the largest reduction of network redundancy level occurs at 10% capacity reduction (See the difference between $NRI3_{in}$ calculated for full capacity and $NRI3_{in}$ for 10% capacity reduction) under different departure rates. Figure 8 presents the total delay for the full network condition in addition to the reduced capacity scenarios. Figures 7 and 8 indicate that the network redundancy for different network conditions follows an opposite trend as the total delay for the same network conditions. For example at 7:30am, $NRI3_{in}$ and the total delay for the network at: a) full capacity, b) 2% and c) 4% reduction are almost the same. When the network capacity reduction increased to d) 10%, more delay is experienced by the network and $NRI3_{in}$ is lower than the previous cases.

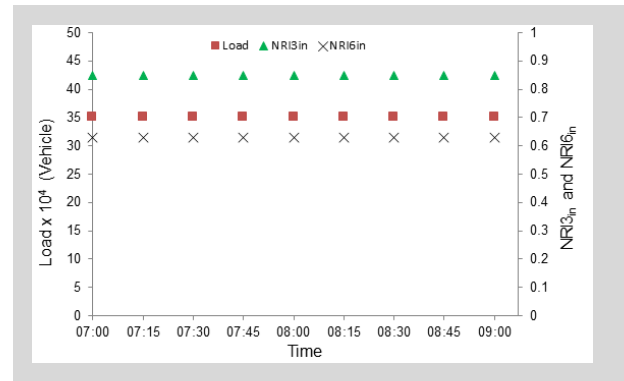


Figure 4 $NRI3_{in}$ and $NRI6_{in}$ under uniform distributed departure rates.

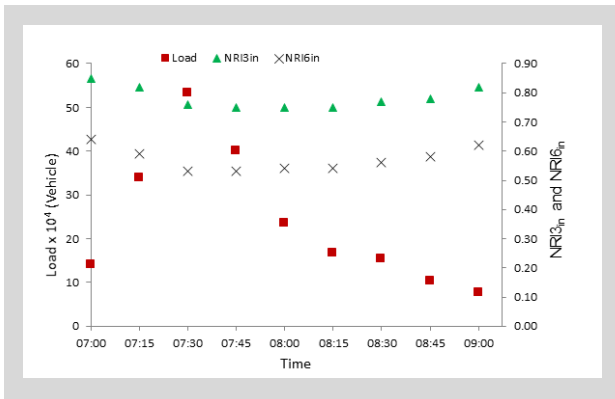


Figure 5 NRIs and network load under different departure rates.

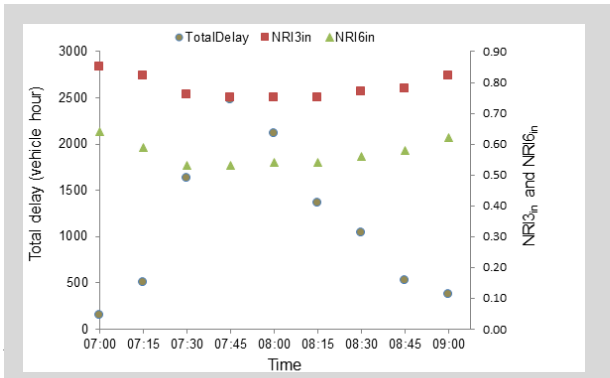


Figure 6 NRI_{3in} and NRI_{6in} and total delay under different departure rates

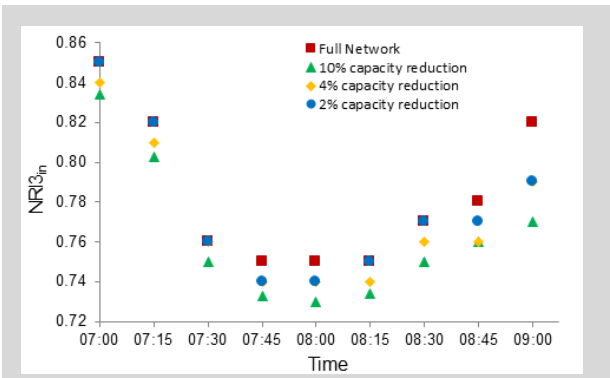


Figure 7 NRI under different departure rates and network capacity.

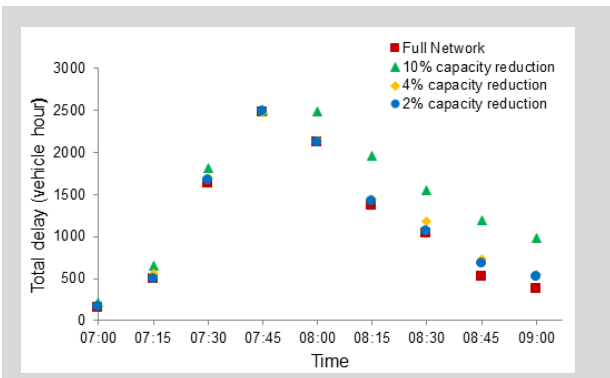


Figure 8 Total delay under different capacity reduction.

4.2. Case Study 2: Junction 3A in M42

Junction 3a in M42 motorway shown in Figure 9 was also employed to investigate the applicability of the proposed redundancy indices to reflect real life conditions. The choice of Junction 3a in M42 is due to the fact that the junction was a part of Active Traffic Management (ATM) scheme by the Highways Agency in 2006, therefore it is possible to study the variation of redundancy under different conditions. The scheme has enhanced the performance of M42 between J3a and J7 by the temporary usage of the hard shoulder to increase the route capacity from 3 lanes (3L) to 4 lanes (4L), jointly with the use of variable mandatory speed limits (VMSL) during periods of peak demand (Sultan *et al.* 2008b). In this study, four time periods were chosen to check the scheme effectiveness i.e. from October 2002 to April 2003 (NO-VMSL), from January 2006 to April 2006 (3L-VMSL), from October 2006 to April 2007 (4L-VMSL), and from January 2007 to April 2007 (4L-VMSL), as indicated in Table 7. According to Sultan *et al.* (2008a), the period October 2006 to April 2007 could be a suitable period to represent the influence of the full scheme, 4 lanes jointly with variable mandatory speed limits (4L-VMSL). Furthermore, the period October 2002 to April 2003 represent the pre-scheme period (NO-VMSL). Furthermore, the periods January 2006 to April 2006 and January 2007 to April 2007 could be implemented to compare between 3L-VMSL and 4L-VMSL, respectively.

Table 5 Summary of r of various redundancy indices with junction delay (JD) and volume capacity ratio (v/c).

| Redundancy index | Junction Type | | | | | | | |
|------------------|----------------|-------|-------------------|-------|---------------------|-------|---------------------|-------|
| | Equal priority | | Give way junction | | Signalized junction | | Roundabout junction | |
| | JD | v/c | JD | v/c | JD | v/c | JD | v/c |
| $RI2_{in}$ | 0.87 | 0.66 | 0.49 | 0.50 | 0.69 | 0.85 | 0.87 | 0.90 |
| $RI3_{in}$ | 0.89 | 0.77 | 0.82 | 0.70 | 0.70 | 0.63 | 0.85 | 0.72 |
| $RI6_{in}$ | 0.90 | 0.77 | 0.81 | 0.78 | 0.71 | 0.71 | 0.85 | 0.63 |

Table 6 $RI3_{in}$ and $RI6_{in}$ values for selected nodes in road transport network of Delft city.

| Node number | inbound links | | | | Junction delay (Veh/min) | Junction volume capacity ratio | $RI3_{in}$ | $RI6_{in}$ |
|-------------|--------------------|------------------------|--------------------|------------------------------|--------------------------|--------------------------------|------------|------------|
| | Link flow (veh/hr) | Link capacity (veh/hr) | Link speed (km/hr) | Link free flow speed (km/hr) | | | | |
| 5001 | 198 | 1800 | 50 | 50 | 0 | 0.07 | 1 | 1 |
| | 41.04 | 1800 | 50 | 50 | | | | |
| 6856 | 773 | 1200 | 29.86 | 35 | 23.53 | 0.26 | 0.91 | 0.88 |
| | 142 | 1200 | 35 | 35 | | | | |
| | 32 | 1200 | 35 | 35 | | | | |
| 6983 | 293 | 2200 | 70 | 70 | 219.33 | 0.56 | 0.75 | 0.67 |
| | 1844 | 2200 | 55.4 | 70 | | | | |
| | 1538 | 2200 | 61.8 | 70 | | | | |
| 7094 | 1483 | 1800 | 35.7 | 50 | 341.72 | 0.35 | 0.81 | 0.79 |
| | 225 | 1500 | 39.98 | 40 | | | | |
| | 88 | 2800 | 50 | 50 | | | | |

4.2.1 Redundancy index of Junction 3A in M42

The traffic flow parameters (i.e. link flow, speed, capacity and free flow speed), on the attached links of J3a were used to calculate $RI3_{in}$ and junction delay. Data for the analysis had been collected from the journey time database (JTDB) which is part of the Highways Agency Traffic Information System (HATRIS) (Highways Agency 2013).

The database included journey time, speed and traffic count data for the motorway and all-purpose trunk road network in England. Data were provided at 15 minute intervals. For each time period, Sundays and Saturdays were excluded from the analysis to examine varied traffic flow profiles during the weekdays.

Table 7 Time periods considered for scheme effectiveness.

| Comparison Task | Time period |
|-------------------------|--|
| NO-VSML against 4L-VMSL | October 2002 to April 2003 October 2006 to April 2007 |
| 3L-VMSL against 4L-VMSL | January 2006 to April 2006 January 2007 to April 2007 |

Figure 10 shows the correlation between $RI3_{in}$ and delay of J3a for two periods of time, October 2002 to April 2003 in Figure 10(a) and October 2006 to April 2007 in Figure 10(b). Both $RI3_{in}$ and delay were calculated as the average for the total period considered at 15 minute intervals. $RI3_{in}$ for J3a showed very strong correlation with the junction delay for both time periods as depicted from Figure 10, confirming the results from the Delft case study.

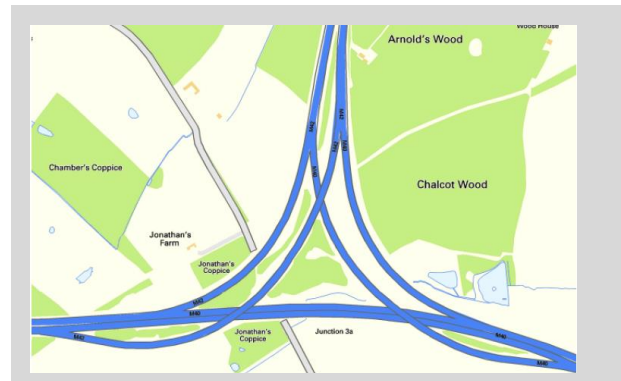
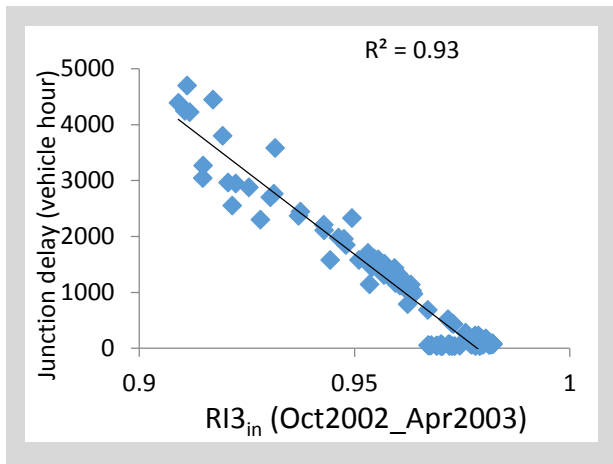
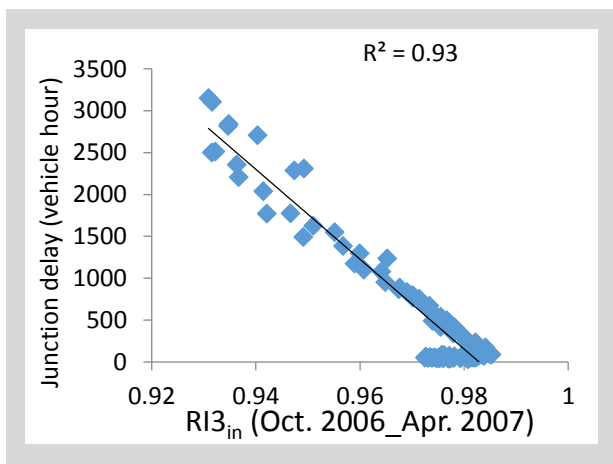


Figure 9 Junction 3a in M42 motorway near Birmingham (© Crown Copyright and database rights 2014; an Ordnance Survey/EDINA-supplied service).



(a) $RI3_{in}$ and junction delay (Oct 2002 to Apr 2003, No-VMSL)



(b) $RI3_{in}$ and junction delay (Oct 2006 to Apr 2007, 4L-VMSL)

Figure 10 $RI3_{in}$ and total delay.

Furthermore, Figure 11 shows the variation of $RI3_{in}$ for the two time periods, October 2002 to April 2003 (pre ATM activation) and October 2006-April 2007 (after the activation of ATM scheme). Comparing $RI3_{in}$ for the time period October 2002 to April 2003 with October 2006 to April 2007 shows that the scheme results in a general improvement in the redundancy index $RI3_{in}$ as depicted from Figure 11. The amount of improvement varies throughout the day, for example at 6:30am (off-peak) both values are very similar, meanwhile there are noticeable improvements between 7:45am to 11:00 pm with different rates.

Figure 12 shows the impact of capacity increase by considering the period between January to April 2006 (3L-VMSL) and the period between January to April 2007 (4L-VMSL). A little improvement in $RI3_{in}$ due to the use of the hard shoulder, especially the morning peak is observed. However, the ATM scheme has attracted more traffic flow (as shown in Figure 13) for both periods that could negatively affect the improvement of $RI3_{in}$.

Conclusions

The main aim of this paper was to introduce a redundancy index for various nodes in road transport networks

that is able to cover both static and dynamic aspects of redundancy. The static aspect of redundancy refers to the existence of alternative paths to a certain node whereas the dynamic aspect covers the issues related to the availability of spare capacity under different network loading and level of service such as the relative average speed. The proposed technique is based on the entropy concept owing to its ability to measure the configuration of a system in addition to being able to model the uncertainties inherent in road transport network. In contrast with previous investigations on redundancy in water systems based on one system characteristic, a number of redundancy indices were developed from combinations of link characteristics to enhance their correlations with the junction delay and the volume capacity ratio.

For each proposed redundancy index two values are calculated (i.e. outbound redundancy and inbound redundancy indices) to quantify the redundancy level of each node in the network. It was found that none of the outbound redundancy indices correlated well with the junction delay or junction volume capacity ratio. Consequently, the analysis focused on the inbound redundancy indices as they were able to reflect the variations in topology of the nodes (e.g. number of incident links) and the variation in link speed. However, further research is recommended to investigate the impact of the outbound links on the junction redundancy index. A network redundancy index is also developed by aggregating a weighted redundancy index for all the nodes.

Two case studies based on a synthetic road transport network of Delft city and Junction 3A in M42 motorway near Birmingham are considered to test the ability of the redundancy indices to reflect various network conditions and demand variation. Each proposed redundancy index was assessed against the junction delay and volume capacity ratio and consequently two redundancy indices based on combined relative link speed and relative link spare capacity were chosen. Furthermore, the suitability of each redundancy index relies on the junction type based on analysis of various junction types in the synthetic road transport network of Delft city. The two chosen redundancy indices responded well to the variation in demand under the same network conditions as well as supply variation, for example network capacity reduction.

The proposed redundancy indices could be a potential tool to identify the optimal design alternatives during the planning stage of the network junctions in addition to the best control and management policies under disruptive events or for daily operation of the road transport network.

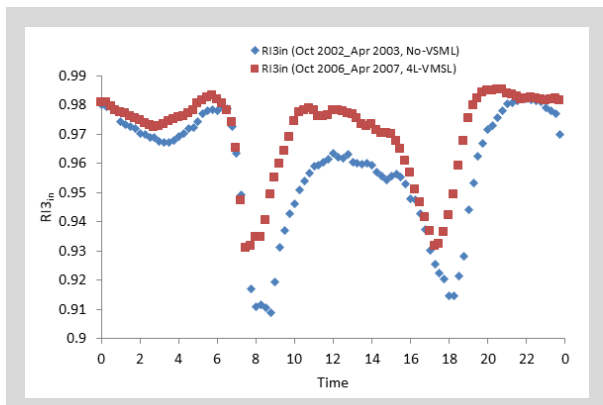


Figure 11 $RI3_{in}$ for the time periods October 2002 to April 2003 and October 2006 to April 2007.

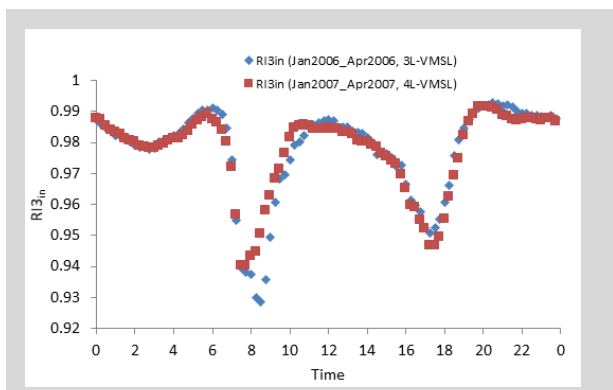


Figure 12 $RI3_{in}$ for the time periods January to April 2006 and January to April 2007.

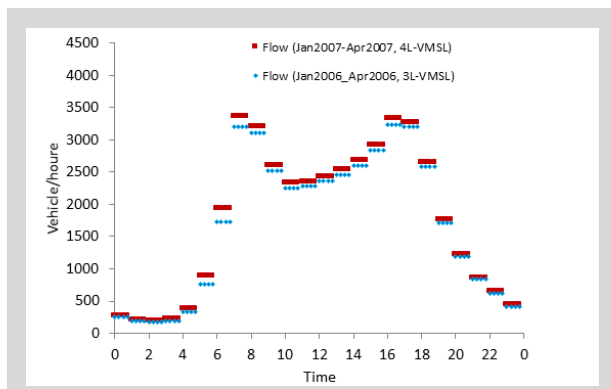


Figure 13 Variation of traffic flow for the time periods January to April 2006 and January to April 2007.

References

- Allesina, S., Azzi, A., Battini, D., Regattieri, A. 2010. Performance measurement in supply chains: new network analysis and entropic indexes. *International Journal of Production Research*, 48, 2297-2321.
- Andreson, W.P., Maoh, H., Burkre, C. 20011. Assessing risk and resilience for transportation infrastructure in Canada. *Canadian Transportation Research Forum: Proceedings of 46th annual conference*, May-June 2011; 298-312.
- Awumah, K., Goulter, I., Bhatt, S. 1991. Entropy-based redundancy measures in water distribution network design. *J. Hydraulic Engrg., ASCE*, 117, 595–614.
- Boccaletti, S., Latora, V., Moreno, Y., Chavez, M., Hwang, D. U. 2006. *Complex networks: Structure and dynamics*. Physics Reports, 424, 175-308.
- Corson, F. 2010. Fluctuations and redundancy in optimal transport networks. *Phys. Rev. Lett*, 104, 1-3.
- DfT, Department for Transport. 2011. Road network policy consultation. Available: www.gov.uk/government/uploads/system/uploads/attachment_data/file/2439/roadnetworkconsultation.pdf. [Accessed 10-05-2014].
- Downer, J. 2009. When failure is an Option: Redundancy, reliability and regulation in complex technical systems. Technical Report Discussion Paper 53, Centre for Analysis of Risk and Regulation (CARR)
- El-RASHIDY, R. A., Grant-Muller, S. M. (2014), “An assessment method for highway network vulnerability”, *Journal of Transport Geography*, 34, 34–43.
- Erath, A., Löchl, M., Axhausen, K. W. 2009. Graph-Theoretical Analysis of the Swiss Road and Railway Networks Over Time. *Networks and Spatial Economics*, 9, 379-400.
- eTN. 2010. The tourism industry implications of the Eyjafjallajökull Volcano eruption [Online]. eTN-Global Travel Industry News. Available: <http://www.eturbonews.com/15558/tourism-industry-implications-eyjafjallajokull-volcano-eruption> [Accessed 7-10-2013].
- Haimes, Y. 2009. On the Definition of Resilience in Systems. *Risk Analysis*, 29(4), 498–501.
- Highways Agency, 2013, HATRIS JTDB Data Guide V7: status in January 2013, <https://jtdb.hatris.co.uk/%5CHATRIS-DataGuideV7.pdf> [Accessed 17-12-2013].
- Hoshiya, M., Asce, M., Yamamoto, K. 2002. Redundancy index of lifeline systems. *Journal of engineering mechanics*, 128, 961-968.
- Hoshiya, M., Yamamoto, K., Ohno, H. 2004. Redundancy index of lifeline for mitigation measures against seismic risk. *Probabilistic Engineering Mechanics*, 19, 205-210.
- Hyder 2010. Network Resilience and Adaptation: Phase 1 Final Report. Highway Agency.
- Immers, B., Stada, J., Yperman, I., Bleukx, A. 2004. Towards robust road network structures. *Slovak Journal of civil engineering*, XII , 10-17.
- Javanbarg, M. B., Takada, S. 2007. Redundancy model for water supply systems under earthquake environments. The 5th International Conf. on Seismology and Earthquake Engineering, May 2007 Tehran, Iran.
- Jenelius, E. 2009. Network structure and travel patterns: explaining the geographical disparities of road network vulnerability. *Journal of Transport Geography*, 17, 234-244.
- Jenelius, E. 2010. Redundancy importance: Links as rerouting alternatives during road network disruptions. *Procedia Engineering*, 3, 129-137.
- Kanno, Y., Ben-Haim, Y. 2011. Redundancy and Robustness, or When Is Redundancy Redundant? *Journal of Structural Engineering*, 137, 935-945.
- Koc, Y., Warnier, M., Kooij, R. E., Brazier, F. M. 2013. An entropy-based metric to quantify the robustness of power grids against cascading failures. *Safety Science*, 59, 126–134.
- Lhomme, S., Serre, D., Diab, Y., Laganier, R. 2013. Analyzing resilience of urban networks: a preliminary step towards

- more flood resilient cities. *Nat. Hazards Earth Syst. Sci.*, 13, 221–230.
- Miao, X., Xi, B., Guan, M., Tang, Y. H. 2011. Route entropy based capacity reliability assessment and application in multi-objective satisfactory optimization of logistics network. *Scientific Research and Essays*, 6, 3335-3343.
- Nagata, S., Yamamoto, K. 2004. Strategy of water supply network restoration with redundancy index. The 13th World Conference on Earthquake Engineering (13 WCEE), 1-6 August 2004, Vancouver, B.C., Canada.
- Ortúzar, J., Willumsen, L. G. 2011. *Modelling transport*, United Kingdom, John Wiley & Sons, Ltd.
- Randles, M., Lamb, D., Odat, E., Taleb-Bendiab, A. 2011. Distributed redundancy and robustness in complex systems. *Journal of Computer and System Sciences*, 77, 293-304.
- Rodrigue, J. P., Comtois, C., Slack, B. 2009. *The geography of transport systems*, Routledge.
- Shannon C. E., 1948. The mathematical theory of communication, *Bell system Tech. J.*, 27(3), 379-423, and 623-659.
- Snelder, M., Van Zuylen, H. J., Immers, L. H. 2012. A framework for robustness analysis of road networks for short term variations in supply. *Transportation Research Part A: Policy and Practice*, 46, 828-842.
- Streeter, L. C. 1992. Redundancy in organizational systems. *Social Service Review*, 66, 97-111.
- Sultan, B., Meekums, R., Brown, M. 2008a. The impact of active traffic management on motorway operation. *Road Transport Information and Control - RTIC 2008 and ITS United Kingdom Members' Conference*, IET, 2008. 1-8.
- Sultan, B., Poole, A., Meekums, R., Potter, R. 2008b. *ATM Monitoring and Evaluation, 4-Lane Variable Mandatory Speed Limits 12 Month Report (Primary and Secondary Indicators)*. Department of Transport (DfT).
- Sun, L., Rong, J., Yao, L., Xu, H., Liu, H. 2011. Estimation of transfers in a terminal. *Journal of Urban Planning and Technology*, 5, 303-315.
- Swanson, G. A., Bailey, K. D., Miller, J. G. 1997. Entropy, Social Entropy and Money: A Living Systems Theory Perspective. *Systems Research and Behavioral Science*, 14, 45-65.
- Wardrop, J.G. 1952. Some theoretical aspects of road traffic research. *Proceedings of the Institution of Civil Engineers, Part II*, 1, pp. 325-378.
- Wilson, A. G. 1970. The Use of the Concept of Entropy in System Modelling. *Operational Research Quarterly* (1970-1977), 21, 247-265.
- Yazdani, A., Jeffrey, P. 2012. Applying network theory to quantify the redundancy and structural robustness of water distribution system. *Journal of Water Resources Planning and Management* 138, 153-161.

